Int J Adv Manuf Technol (2016) 84:2301–2318
DOI 10.1007/s00170-015-7791-x

ORIGINAL ARTICLE

Sensitivity analysis of machining accuracy of multi-axis machine tool based on POE screw theory and Morris method

Qiang Cheng[1,2] · Qiunan Feng[1] · Zhifeng Liu[1] · Peihua Gu[3] · Guojun Zhang[2]

Received: 20 April 2015 / Accepted: 31 August 2015 / Published online: 28 September 2015

Abstract The geometric errors have a significant effect on the machining accuracy of multi-axis machine tool. Because of their complex inter-coupling, the process to control these geometric errors and then to improve the machining accuracy on this basis is recognized as a difficult problem. This paper proposes a method based on the product of exponential (POE) screw theory and Morris approach for volumetric machining accuracy global sensitivity analysis of a machine tool. When a five-axis machine tool is chosen as an example, there are five screws to represent the six basic error components of each axis (in an original way) according to the geometric definition of the errors and screws. This type of POE model is precise and succinct enough to express the relation of each of the components as the Morris method is based on the elementary effect (EE). The method can compare incidence of these errors and be used to describe the nonlinear relationship by less calculated amount in a global system. Based on the POE modelling, the Morris method is adopted to identify the key geometric errors which have a greater influence on the machining accuracy by global sensitivity analysis. Finally, according to the results obtained from analysis, suggestions, and guidelines are provided to adjust and modify the machine tool components to improve the machining accuracy economically.

Keywords Machine tool · Screw theory · Geometric error · Morris method · Sensitivity analysis

✉ Zhifeng Liu
lzfbjut@gmail.com

[1] College of Mechanical Engineering and Applied Electronics Technology, Beijing University of Technology, Beijing 100124, China

[2] State Key Lab of Digital Manufacturing Equipment & Technology, Huazhong University of Science and Technology, Wuhan 430074, China

[3] Department of Mechatronics Engineering, Shantou University, Shantou, Guangdong, China 515063

1 Introduction

Multi-axis CNC machine tool is widely used in the manufacturing industry. Because of its high efficiency and capability in machining complex surfaces, it is one of the most important components in the modern manufacturing facilities [1, 2]. Machining accuracy is a key factor in evaluating the capability of multi-axis machine tools, and it is affected by geometrical, thermal, kinematic, stiffness, and cutting tool deflection errors [3–5]. Among these, the geometric error has major effect on the machining accuracy [6], accounting for 40 % of all errors [7], especially when relatively high precision is a requirement [8]. The geometric errors are systematic or repeatable, time-invariant and can be measured and stored [9, 10].

Generally, there are two ways to improve the geometric accuracy of machine tools: (1) design and manufacture for precision and (2) error compensation [11]. The error modeling aims to establish a map from the geometric source errors to the position errors of machine tool. It is the common premise of precision design and error compensation [12] and can lay a foundation for the error compensation. Over the past several decades, research was focused on the error modeling of machine tools along with the modeling methods for geometric errors, especially the influence of geometric errors on three-axis machine tools [13].

The modeling methods for geometric errors have been developed from different perspectives, and these include geometric modeling method, error matrix method (EMM), quadratic

model method, mechanism modeling method, rigid body kinematics method [14, 15], and multi-body system kinematics theory [16]. Fan et al. [17] proposed kinematics of a multi-body system theory (MBS) by adding movement and positioning error terms. This approach allowed development of a generalized kinematic model, applicable to the NC machine tools. The POE model has been widely used in recent years in the field of robotics. Because this model can express the kinematic chain of a robot clearly, it is more suitable to describe the motion of robot according to its geometric property, and it is a zero reference position method [18]. Moon et al. studied the geometric error modeling and compensation for the machine tools using the screw theory [19]. They expressed the basic error components of each joint as a modular error screw and defined modular error screws and motion screws of the joints with respect to a global reference frame. Despite all this work, they merely used this method to establish the three-axis machine tool model excluding the rotation axis.

There are several inter-coupling [20] geometric errors in a multi-axis machine tool, but the method to determine the influence of different geometric errors on the machining accuracy currently remains as a difficult problem in the design of machine tools. The sensitivity analysis is one approach to identify and quantify the relationships between input and output uncertainties [21]. Different strategies have been applied as found in the literature [22], which are typically classified into two categories: global sensitivity analysis (GSA) [23, 24] and the local sensitivity analysis (LSA). The LSA which emphasizes the effect of small parameter variations on the model responses is used to determine the changes in model response with an individual parameter. The GSA is applied to understand how the model response varies with model parameters and to determine interaction strengths among the parameters [25]. However, the LSA can only inspect one point at a time, and the sensitivity index of a specific parameter is dependent on the central values of the other parameters.

With rigorous sensitivity analysis (SA) of geometric errors, the most critical geometric errors can be identified and can be strictly controlled, and thus, the machining accuracy of machine tool can be significantly improved [26]. The most recent research work is found to focus on the application of LSA. However, only three special configurations were selected to perform the analysis, which probably were insufficient. Cheng et al. [27] considered the stochastic characteristics of geometric errors and used the Sobol' global sensitivity analysis method to identify the key geometric errors of machine tool. The screening method initially developed by Morris [28] and later modified by Campolongo et al. [29] is known as elementary effects method. This method has been successfully applied in hydrological [30] and ecological disciplines [31] and also in environmental engineering [32], as it can estimate the parameter interactions by considering both the mean and variance of the elementary effects with far less computational expenses [33].

To overcome the drawbacks of local sensitivity analysis and identify the critical geometric errors of machine tools more reasonably, this paper proposes a new analytical method for the identification of key geometric errors of multi-axis machine tool based on POE screw theory and Morris global sensitivity analysis. There are two major contributions from this paper: One is the volumetric error modeling of five-axis machine tool by POE screw theory. The other is that the random characteristic of geometric errors is taken into consideration, and the Morris method is introduced to identify the key geometric errors of machine tool. The method of Morris can estimate the parameter interactions by considering both the mean and variance of the elementary effects.

The rest of this paper is organized as follows. Section 2 gives the framework of the proposed method. In Sections 3 and 4, the modeling of the volumetric machining accuracy based on geometric errors is presented. The analytical method based on Morris method to identify the critical geometric errors is presented and a vertical machining center is selected as an example for experimental verification of the analytical method in Section 5. The conclusions are presented in Section 6.

2 Framework of the proposed approach

In this paper, two major innovations are presented. One is that POE screw theory is used for error modeling, especially for the rotation axis error modeling. The other is Morris global sensitivity. With experimentation and simulation, the useful results were obtained and successfully analyzed. The approach presented in this paper consisting of three main steps is summarized in Fig. 1.

3 Geometric error modeling for five-axis machine tool

3.1 Screw theory and POE modelling

The screw theory forms the basis for error modelling. In this expression, ω denotes the instantaneous angular velocity and $\boldsymbol{v}$ is linear velocity. In the Plücker coordinate system, the unit screw can be expressed as:

$$\$=\left[\omega^T \; v^T\right]^T = \left[\omega_1, \omega_2, \omega_3, v_1, v_2, v_3\right]^T \tag{1}$$

If it is assumed that, "$\hat{\$}$ " can express any motion of the rigid body:

$$\hat{\$} = \begin{bmatrix} \hat{\omega} & v \\ 0 & 0 \end{bmatrix} \tag{2}$$

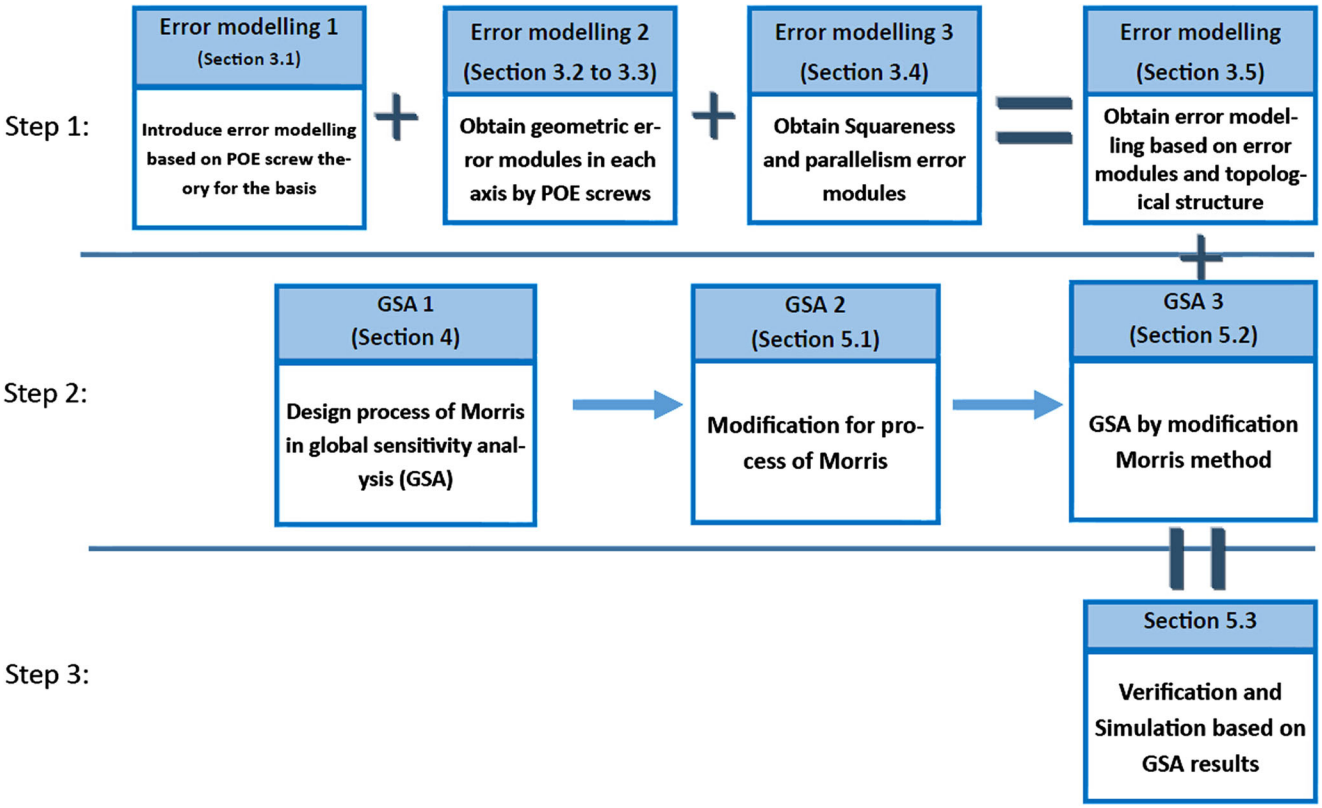

Fig. 1 Framework of the proposed approach

where, $\upsilon=[v_1,v_2,v_3]^T$ and $\hat{\boldsymbol{\omega}}$ is a skew-symmetric matrix.

The composite motion of the rigid body contains rotation and translation [34]. Assuming that the vector between the rigid body coordinate system and reference coordinate system is q, the homogeneous transformation matrix of the rigid body is given by:

$$\boldsymbol{T} = e^{\hat{\$}\theta} = \begin{bmatrix} R & \mathrm{q} \\ 0 & 1 \end{bmatrix} \tag{3}$$

The exponential matrix of the screw is also the corresponding homogeneous transformation matrix, namely $\boldsymbol{T} = e^{\hat{\$}\theta}$. There are two extreme situations in motions that is only translational motion ($\boldsymbol{\omega}=0$) or rotational motion ($\boldsymbol{\omega}\neq 0$) [15]:

If $ is unit screw, the motion of rigid body can be written as follows:

$$\boldsymbol{T}=\boldsymbol{e}^{\hat{\$}\theta} = \begin{cases} \begin{bmatrix} I_{3\times 3} & \vec{v} \\ 0 & 1 \end{bmatrix} & if \|\omega\| = 0 \\ \begin{bmatrix} e^{\hat{\omega}\theta} & \left(I - e^{\hat{\omega}\theta}\right)\left(\dfrac{\vec{\omega}\times\vec{v}}{(\|\omega\|\theta)^2}\right) + \dfrac{\vec{\omega}\vec{\omega}^T\vec{v}}{(\|\omega\|\theta)^2} \\ 0 & 1 \end{bmatrix} & if \|\omega\| \neq 0 \end{cases} \tag{4}$$

where, $e^{\hat{\omega}\theta}$ can be expanded by trigonometric series method:

$$e^{\hat{\omega}\theta} = I + \frac{\hat{\omega}}{\|\omega\|}sin\theta + \frac{\hat{\omega}^2}{\|\omega\|^2}(1-cos\theta) \tag{5}$$

For the case when $\|\boldsymbol{\omega}\|\neq 0$, the rotation angle $\boldsymbol{\theta}=\sqrt{\omega_1^2+\omega_2^2+\omega_3^2}$. Otherwise, the translational distance $\boldsymbol{\theta}=\sqrt{v_1^2+v_2^2+v_3^2}$. A given point is defined by different coordinates in different coordinate systems, and the transformation matrix of these coordinate systems is used to express the relationship between the coordinates. A screw is similar to a point. The coordinates of a screw in different coordinate systems are different. The adjoint matrix, in different coordinate frames for the screws, is used to obtain the different expressions. The transformation matrix of rigid body motion screw $\boldsymbol{\theta}$$ can be expressed by Eq. (2) and the adjoint matrix of transformation matrix is given by Eq. (6:)

$$\boldsymbol{Adj}\left(\boldsymbol{e}^{\theta\hat{\$}}\right) = \begin{bmatrix} R & 0 \\ \hat{q} & R \end{bmatrix} \tag{6}$$

The properties of adjoint matrix can be expressed in the form shown by Eqs. (7) and (8) [27].

$$\hat{\boldsymbol{\$}}_{\boldsymbol{I}} = Adj\left(e^{\theta\hat{\$}_1}\right)\$_2 = e^{\theta\hat{\$}_1}\hat{\$}_2\left(e^{\theta\hat{\$}_1}\right)^{-1} \tag{7}$$

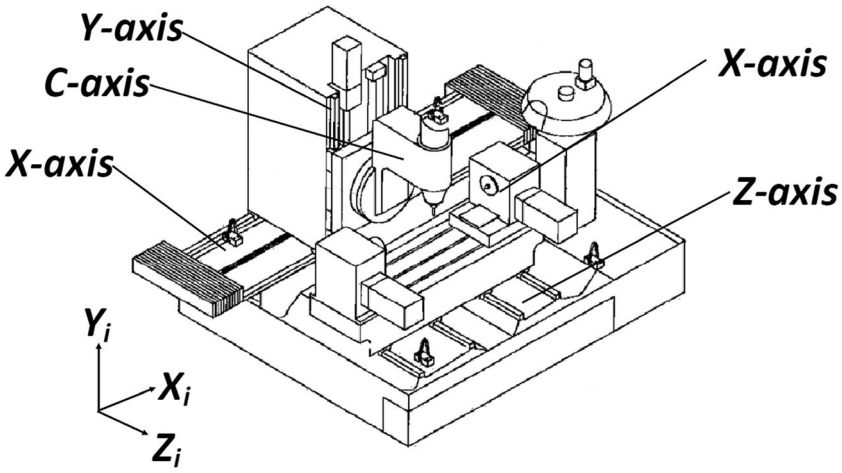

Fig. 2 Illustration of a five-axis machine tool

$$\boldsymbol{e}^{\hat{\boldsymbol{S}}_I} = e^{e^{\theta\hat{S}_1}\hat{S}_2\left(e^{\theta\hat{S}_1}\right)^{-1}} = e^{\theta\hat{S}_1}e^{\hat{S}_2}\left(e^{\theta\hat{S}_1}\right)^{-1} \tag{8}$$

Moreover, the POE screw theory modelling can be adopted to express the forward kinematics of an open chain robot. For an n-DOF(degrees of freedom) robot, the forward kinematics can be written as shown by Eq. (9) [35].

$$\boldsymbol{T} = e^{\hat{S}_1\theta_1}\cdot e^{\hat{S}_2\theta_2}\cdots e^{\hat{S}_n\theta_n}\cdot \boldsymbol{T}(0) \tag{9}$$

The matrix $\boldsymbol{T}(0)$ represents the initial transformation matrix. Equation (9), which represents the POE model, can also be used in error modeling of the machine tools.

3.2 Geometric error for five-axis machine tool

In the previous section, the POE screw theory modelling for rigid body is introduced in general terms. In this section, the POE screw theory modelling is applied to establish the volumetric error model of a five-axis machine tool. The motion of each axis and the geometric errors of machine tool can be described by a screw and POE modelling. The squareness and parallelism errors are represented in detail with the POE model. The screws can be used to explain the squareness errors clearly according to their geometric properties, and the model can be used to describe the rigid body transformation.

Each component of the machine tool which is represented in the global reference coordinate system has motion screws and error screws, such as the axes, spindle, and milling head. These screws of these parts make up the kinematic chain and are basic to the topological structure. The geometric error from the workpiece obtained by the coordinate system of the working table is chosen as the reference coordinate system. The exponential matrixes of error screws and motion screws are multiplied to obtain the geometric error model by the analysis of topological structure. In this paper, the five-axis machine tool is considered as an example to introduce the method for volumetric machining accuracy global sensitivity analysis. The five-axis machine tools are becoming increasingly popular in high-accuracy and processing of abnormal parts. The schematic diagram of the five-axis machine tool is shown in Fig. 2.

In general, a five-axis machine tool has 39 error components in total, which include the linear positioning errors, straightness errors, angular errors, squareness errors, and parallelism errors. These errors are listed in the Table 1. In this list, δ is the linear error, and ε is the angular error; δ_{yx} is the linear error in $\boldsymbol{y}$ direction while the X-axis is in motion. Here, the definitions and relationships of S_{AY} and S_{CY} are similar to those of parallelism errors. Furthermore, they are considered as repetitive and unimportant error terms and for this reason are not explained in detail in this paper

Table 1 Error components of five-axis machine tool

Errors	Number of errors	Symbols
Linear positioning errors	5	δ_{xx}, δ_{yy}, δ_{zz}, δ_{xA}, δ_{zC}
Horizontal straightness errors	5	δ_{yx}, δ_{zy}, δ_{xz}, δ_{yA}, δ_{xC}
Vertical straightness errors	5	δ_{zx}, δ_{xy}, δ_{yz}, δ_{zA}, δ_{yC}
Roll angular errors	5	ε_{xx}, ε_{yy}, ε_{zz}, ε_{xA}, ε_{zC}
Pitch angular errors	5	ε_{yx}, ε_{zy}, ε_{xz}, ε_{yA}, ε_{xC}
Yaw angular errors	5	ε_{zx}, ε_{xy}, ε_{yz}, ε_{zA}, ε_{yC}
Squareness errors	5	S_{xy}, S_{yz}, S_{xz}, S_{AY}, S_{CY}
Parallelism errors	4	PY_{xA}, PZ_{xA}, PX_{zC}, PY_{zC}

3.3 Geometric errors modelling by screws

The five-axis machine tool in general has three translational and two rotational motions. The unit motion screws can be expressed as:

$$\$_b = \left[r_x, 0, r_z, s_x, s_y, s_z\right]^T$$

in which,$\boldsymbol{s}=[s_x,s_y,s_z]^T$ represents the unit vector in direction of motion of the translational axis;$\boldsymbol{r}=[r_x,0,r_z]^T$ represents the unit vector of rotation about the translation axis.

The exponential matrix of five-axis machine tool motion which is $e^{\$_b}$ can be expressed as:

$$\boldsymbol{e}^{\$_b} = \begin{bmatrix} 1 & -r_z & 0 & s_x \\ r_z & 1 & -r_x & s_y \\ 0 & r_x & 1 & s_z \\ 0 & 0 & 0 & 1 \end{bmatrix}$$

For instance, with regard to *X*-axis, the unit motion screw is $\$_x$. The symbol *x* represents the displacement of *X*-axis, and the same applies to *Y*-axis, *Z*-axis, *A*-axis, and *C*-axis. $\$_y$ and $\$_z$ represent the motion screws of *Y*-axis and *Z*-axis, respectively, and the symbols *y* and *z* represent the displacement of each axis. $\$_A$ and $\$_C$ represent the rotation screws. The symbols A and C represent angle of rotation about the *A*-axis and *C*-axis, respectively. Then, the corresponding exponential matrixes are the ideal transformation matrixes of each axis. The motion screws and exponential matrixes are as follows:

$$\begin{aligned} \$_x &= [0,0,0,1,0,0]^T \\ \$_y &= [0,0,0,0,1,0]^T \\ \$_z &= [0,0,0,0,0,1]^T \\ \$_A &= [1,0,0,0,0,0]^T \\ \$_C &= [0,0,1,0,0,0]^T \end{aligned}$$

$$\boldsymbol{e}^{x\$_x} = \begin{bmatrix} 1 & 0 & 0 & \mathrm{x} \\ 0 & 1 & 0 & 0 \\ 0 & 0 & 1 & 0 \\ 0 & 0 & 0 & 1 \end{bmatrix};\quad \boldsymbol{e}^{y\$_y} = \begin{bmatrix} 1 & 0 & 0 & 0 \\ 0 & 1 & 0 & \mathrm{y} \\ 0 & 0 & 1 & 0 \\ 0 & 0 & 0 & 1 \end{bmatrix} \tag{10}$$

$$\boldsymbol{e}^{z\$_z} = \begin{bmatrix} 1 & 0 & 0 & 0 \\ 0 & 1 & 0 & 0 \\ 0 & 0 & 1 & z \\ 0 & 0 & 0 & 1 \end{bmatrix};\quad \boldsymbol{e}^{A\$_A} = \begin{bmatrix} 1 & 0 & 0 & 0 \\ 0 & 1 & -A & 0 \\ 0 & A & 1 & 0 \\ 0 & 0 & 0 & 1 \end{bmatrix}$$

$$\boldsymbol{e}^{C\$_C} = \begin{bmatrix} 1 & -C & 0 & 0 \\ C & 1 & 0 & 0 \\ 0 & 0 & 1 & 0 \\ 0 & 0 & 0 & 1 \end{bmatrix}$$

Due to manufacturing and installation defects, geometric errors are inevitable for each axis. In general, the six error components can be used to describe the geometric errors of a moving axis since a rigid body has six degrees of freedom [22], which include three translational errors and three rotational errors. Moon et al. described the six error components as modular error components using the screw theory [28]. They defined the modular error screw, $\boldsymbol{m_e}\$_{\boldsymbol{e}}$ as follows:

$$\boldsymbol{m_e}\$_{\boldsymbol{e}} = \left[\varepsilon_x, \varepsilon_y, \varepsilon_z, \delta_x, \delta_y, \delta_z\right]^T$$

Considering the *X*-axis part as an example, the first group contains linear positioning error δ_{xx} and roll angular error ε_{xx}, for which the corresponding screw is $\$_{\boldsymbol{xx}}$. The second group consists of horizontal straightness error δ_{yx} and pitch angular error ε_{yx}, for which the corresponding screw is $\$_{\boldsymbol{yx}}$. The third group consists of vertical straightness error δ_{zx} and yaw angular error ε_{zx}, for which the corresponding screw is $\$_{\boldsymbol{zx}}$.

The screws, $\$_{\boldsymbol{xx}}$, $\$_{\boldsymbol{yx}}$ and $\$_{\boldsymbol{zx}}$ can be written as follows:

$$\$_{\boldsymbol{xx}} = [\varepsilon_{xx}, 0, 0, \delta_{xx}, 0, 0]^T \tag{11}$$

$$\$_{\boldsymbol{yx}} = \left[0, \varepsilon_{yx}, 0, 0, \delta_{yx}, 0\right]^T \tag{12}$$

$$\$_{\boldsymbol{zx}} = [0, 0, \varepsilon_{zx}, 0, 0, \delta_{zx}]^T \tag{13}$$

The corresponding exponential matrices represent the transformation of these three screws, and $\boldsymbol{e}^{\hat{\$}_{xe}}$ represents the transformation matrix of geometric errors for X-axis as shown by Eq. (14):

$$\boldsymbol{e}^{\hat{\$}_{xe}} = e^{\hat{\$}_{xx}} \cdot e^{\hat{\$}_{yx}} \cdot e^{\hat{\$}_{zx}} \tag{14}$$

The error modelling for *X*-axis can be written as:

$$\boldsymbol{T^x} = e^{x\hat{\$}_x} \cdot e^{\hat{\$}_{xe}} = e^{x\hat{\$}_x} \cdot e^{\hat{\$}_{xx}} \cdot e^{\hat{\$}_{yx}} \cdot e^{\hat{\$}_{zx}} \tag{15}$$

On a basis similar to the method used for the error modelling of *X*-axis, Fu [13] introduced the motion screws clearly. Here, the error screws of *Y*-axis and *Z*-axis will not be listed in detail. Furthermore, the corresponding geometric error rotation screw models of *A*-axis and *C*-axis can be represented as:

$$\begin{aligned} \$_{\boldsymbol{xA}} &= [\varepsilon_{xA}, 0, 0, \delta_{xA}, 0, 0]^T \\ \$_{\boldsymbol{yA}} &= \left[0, \varepsilon_{yA}, 0, 0, \delta_{yA}, 0\right]^T \\ \$_{\boldsymbol{zA}} &= [0, 0, \varepsilon_{zA}, 0, 0, \delta_{zA}]^T \end{aligned} \tag{16}$$

$$\boldsymbol{e}^{\hat{\$}_{Ae}} = e^{\hat{\$}_{xA}} \cdot e^{\hat{\$}_{yA}} \cdot e^{\hat{\$}_{zA}} \tag{17}$$

$$\boldsymbol{T^A} = e^{A\hat{\$}_A} \cdot e^{\hat{\$}_{Ae}} = e^{A\hat{\$}_A} \cdot e^{\hat{\$}_{xA}} \cdot e^{\hat{\$}_{yA}} \cdot e^{\hat{\$}_{zA}}; \tag{18}$$

$$\begin{aligned} \$_{\boldsymbol{xC}} &= [\varepsilon_{xC}, 0, 0, \delta_{xC}, 0, 0]^T \\ \$_{\boldsymbol{yC}} &= \left[0, \varepsilon_{yC}, 0, 0, \delta_{yC}, 0\right]^T \\ \$_{\boldsymbol{zC}} &= [0, 0, \varepsilon_{zC}, 0, 0, \delta_{zC}]^T \end{aligned} \tag{19}$$

$$\boldsymbol{e}^{\hat{\$}_{Ce}} = e^{\hat{\$}_{xC}} \cdot e^{\hat{\$}_{yC}} \cdot e^{\hat{\$}_{zC}} \tag{20}$$

$$\boldsymbol{T^C} = e^{C\hat{\$}_C} \cdot e^{\hat{\$}_{Ce}} = e^{C\hat{\$}_C} \cdot e^{\hat{\$}_{xC}} \cdot e^{\hat{\$}_{yC}} \cdot e^{\hat{\$}_{zC}} \tag{21}$$

3.4 Squareness and parallelism errors modelling

Due to the deviation of actual axis from the ideal axis, the angle between the adjacent axes is not equal to 90°, and this causes squareness error. The squareness errors can be explained as follows: as the *Y*-axis is defined to align with the reference coordinate system, there is no squareness error (for actual *Y*-axis). $\boldsymbol{S_{xy}}$ is the squareness error between *X*-axis and *Y*-axis, $\boldsymbol{S_{yz}}$ is between *Y*-axis and *Z*-axis, and $\boldsymbol{S_{xz}}$ is between *X*-axis and *Z*-axis. The plane formed by actual *X*-axis and *Y*-axis is called the reference *X*–*Y* plane. There is only squareness error $\boldsymbol{S_{xy}}$ for actual *X*-axis; meanwhile, for the actual *Z*-axis, there exist two other squareness errors, which are shown in Fig. 3.

Taking the *X*-axis as an example, the ideal unit motion screw $\boldsymbol{S_{xi}}$ is given by:

$$\$_{xi} = [0,0,0,1,0,0]^T \tag{22}$$

With the squareness error $\boldsymbol{S_{xy}}$, the actual unit motion screw is $\$_{xs}$ and it is given by:

$$\$_{xs} = \left[0,0,0,cos\left(\boldsymbol{S_{xy}}\right),-\sin\left(\boldsymbol{S_{xy}}\right),0\right]^T \tag{23}$$

$e^{x\hat{\$}_{xs}}$, the actual exponential matrix of *X*-axis, can be written as:

$$e^{x\hat{\$}_{xs}} = \begin{bmatrix} 1 & 0 & 0 & x\cos\left(S_{xy}\right) \\ 0 & 1 & 0 & -x\sin\left(S_{xy}\right) \\ 0 & 0 & 1 & 0 \\ 0 & 0 & 0 & 1 \end{bmatrix} \tag{24}$$

Further, the adjoint matrix can be used to represent the coordinate transformation. According to the Eq. (7), the reference coordinate system rotates through an angle about the ideal Z-axis, and this process can be denoted by Eq. (25).

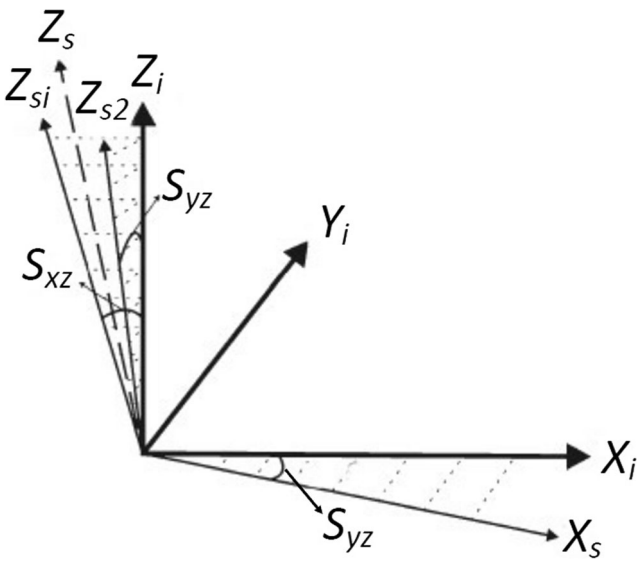

Fig. 3 Three squareness errors in five-axis machine tool

$$\begin{aligned} \$_{xs} &= Adj\left(e^{-S_{xy}\hat{\$}_{zr}}\right)\cdot\$_{xi} \\ \$_{zr} &= [0,0,1,0,0,0]^T \end{aligned} \tag{25}$$

In the above, second subscript ***r*** represents the rotation of the screw about the axis denoted by first subscript which means the nominal axis.

Similarly, the ideal unit motion screw for *Z*-axis is $\$_{zi}$, the actual unit motion screw is $\$_{xs}$, and exponential matrix is $e^{z\hat{\$}_{zs}}$. These can be written as shown in Eq. (26).

$$\begin{aligned} \$_{zi} &= [0,0,0,0,0,1]^T \\ \$_{zs} &= \left[0,0,0,-sin\left(\boldsymbol{S_{xz}}\right),-\sin\left(\boldsymbol{S_{yz}}\right)cos\left(\boldsymbol{S_{xz}}\right),\cos\left(\boldsymbol{S_{yz}}\right)cos\left(\boldsymbol{S_{xz}}\right)\right]^T \\ e^{z\hat{\$}_{zs}} &= \begin{bmatrix} 1 & 0 & 0 & -z\sin\left(\boldsymbol{S_{xz}}\right) \\ 0 & 1 & 0 & -z\cos\left(\boldsymbol{S_{xz}}\right)sin\left(\boldsymbol{S_{yz}}\right) \\ 0 & 0 & 1 & z\cos\left(\boldsymbol{S_{xz}}\right)cos\left(\boldsymbol{S_{yz}}\right) \\ 0 & 0 & 0 & 1 \end{bmatrix} \end{aligned} \tag{26}$$

As in the method of the adjoint matrix coordinate transformation, the reference coordinate system rotates through an angle about the ideal *Y*-axis at the first instance and then rotates through an angle about the ideal *X*-axis. This transformation can be shown by Eq. (27).

$$\$_{zs1} = Adj\left(e^{-S_{xz}\hat{\$}_{yr}}\right)\$_{zi};\quad \$_{zs} = Adj\left(e^{S_{yz}\hat{\$}_{yr}}\right)\$_{zs1} \tag{27}$$

In the above, $\$_{xr}=[1,0,0,0,0,0]^T$ is the unit rotation about ideal *X*-axis and $\$_{yr}=[0,1,0,0,0,0]^T$ is the unit rotation about ideal *Y*-axis.

With regard to the parallelism errors, especially for the rotation of *A*-axis and *C*-axis, a deviation occurs between *X*-axis and *Z*-axis during the installation of machine tool. There are two errors between the actual *A*-axis and ideal *X*-axis, and these are the parallelism error PY_{xA} on *Y*-axis, and PZ_{xA} on *Z*-axis. In a similar way, the two parallelism errors between the actual *C*-axis and ideal *Z*-axis can be shown as illustrated in Fig. 4, in which X_i, Y_i, and Z_i represent ideal axes.

Considering *A*-axis as an example, the ideal rotation unit screw about the *X*-axis is $\$_{Ai}$ and it is given by:

$$\$_{Ai} = [1,0,0,0,0,0]^T \tag{28}$$

With the parallelism errors $\boldsymbol{PY_{xA}}$ and $\boldsymbol{PZ_{xA}}$, the actual unit rotation screw $\$_{As}$ can be shown as:

$$\$_{As} = \left[\cos\left(\boldsymbol{PY_{xA}}\right)cos\left(\boldsymbol{PZ_{xA}}\right),-\sin\left(\boldsymbol{PY_{xA}}\right)cos\left(\boldsymbol{PZ_{xA}}\right),-sin\left(\boldsymbol{PZ_{xA}}\right),0,0,0\right]^T \tag{29}$$

The actual exponential matrix of A-axis $e^{A\hat{\$}_{As}}$ can be written as:

$$e^{A\hat{\$}_{As}} = \begin{bmatrix} 1 & Asin(PZ_{xA}) & -A\sin(PY_{xA})cos(PZ_{xA}) & 0 \\ -Asin(PZ_{xA}) & 1 & -A\cos(PY_{xA})cos(PZ_{xA}) & 0 \\ A\sin(PY_{xA})cos(PZ_{xA}) & A\cos(PY_{xA})cos(PZ_{xA}) & 1 & 0 \\ 0 & 0 & 0 & 1 \end{bmatrix} \quad (30)$$

As in adjoint matrix coordinate transformation method, the reference coordinate system rotates through an angle about the ideal Y-axis at firs and then rotates through an angle about the ideal Z-axis. Equation (31) shows this transformation.

$$\$_{As1} = Adj\left(e^{PY_{xA}\hat{\$}_{zr}}\right)\$_{xi};\ \ \$_{As} = Adj\left(e^{PZ_{xA}\hat{\$}_{yr}}\right)\$_{As1} \quad (31)$$

On a similar basis, the ideal unit rotation screw for C-axis is represented by $\$_{Ci}$, the actual unit rotation screw by $\$_{Cs}$, and exponential matrix is represented by $e^{C\hat{\$}_{Cs}}$. These can be expressed as shown by Eq. (32).

$$\$_{Ci} = [0,0,1,0,0,0]^T \$_{Cs} = [-sin(PY_{zC}), -\sin(PX_{zC})cos(PY_{zC}), \cos(PX_{zC})cos(PY_{zC}), 0, 0, 0]^T$$

$$e^{C\hat{\$}_{Cs}} = \begin{bmatrix} 1 & -C\cos(PX_{zC})cos(PY_{zC}) & -C\sin(PX_{zC})cos(PY_{zC}) & 0 \\ C\cos(PX_{zC})cos(PY_{zC}) & 1 & Csin(PY_{zC}) & 0 \\ C\sin(PX_{zC})cos(PY_{zC}) & -Csin(PY_{zC}) & 1 & 0 \\ 0 & 0 & 0 & 1 \end{bmatrix} \quad (32)$$

As in adjoint matrix coordinate transformation method, the reference coordinate system rotates through an angle about the ideal Y-axis at first and then rotates through an angle around the ideal X-axis. This transformation can be expressed as shown by Eq. (33).

$$\$_{Cs1} = Adj\left(e^{-PY_{zC}\hat{\$}_{yr}}\right)\$_{Zi};\ \ \$_{Cs} = Adj\left(e^{PX_{zC}\hat{\$}_{xr}}\right)\$_{Cs1} \quad (33)$$

3.5 Modelling of volumetric error using topological structure

In this paper, the five-axis machine tool is considered as an example, and its schematic diagram is shown in Fig. 2. The multi-body system (MBS) theory is applied to obtain a detailed topological structure of the machine tool, which is shown in Fig. 5, and it can be applied to the geometric errors POE model.

Under ideal conditions, errors do not exist. The order of modelling is in the following sequence: $C_i \rightarrow X_i \rightarrow Y_i \rightarrow Z_i \rightarrow A_i$. The ideal transformation matrix, namely the ideal POE model, T_i is obtained as:

$$T_i = e^{-c\hat{\$}_{C_i}} \cdot e^{-x\hat{\$}_{X_i}} \cdot e^{-y\hat{\$}_{Y_i}} \cdot e^{z\hat{\$}_{Z_i}} \cdot e^{a\hat{\$}_{A_i}} \quad (34)$$

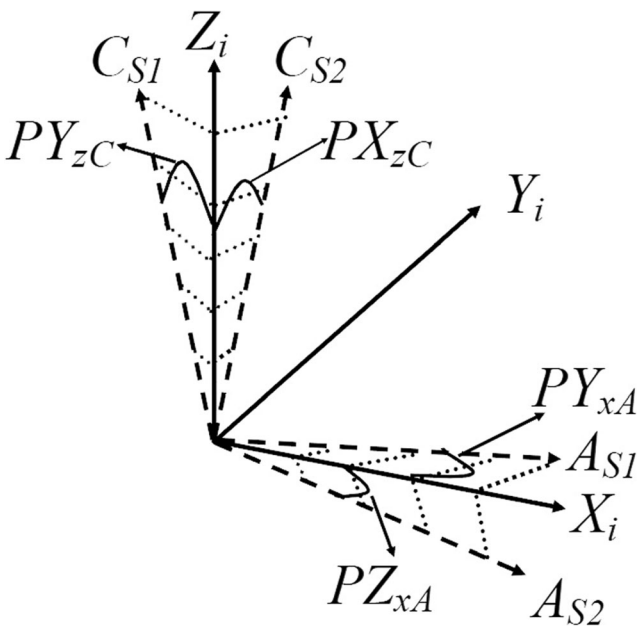

Fig. 4 Four parallelism errors in five-axis machine tool

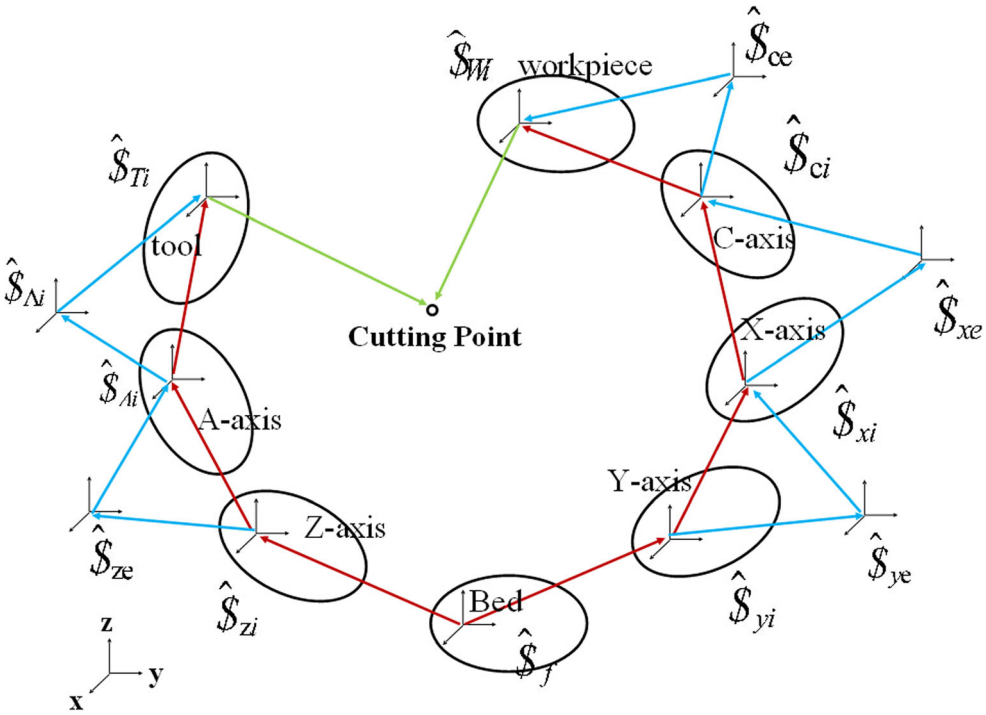

Fig. 5 Topological structure of the five-axis machine tool

With the error screws, squareness errors, parallelism errors, linear errors, and rotation errors, the actual POE model $\boldsymbol{T_a}$ of the machine tool as illustrated in Fig. 5 can be written as Eq. (35):

$$\begin{aligned}\boldsymbol{T_a} &= e^{-\hat{\$}_{Ce}}\cdot e^{-c\hat{\$}_{cs}}\cdot e^{-\hat{\$}_{Xe}}\cdot e^{-x\hat{\$}_{Xs}}\cdot e^{-\hat{\$}_{Ye}}\cdot e^{-y\hat{\$}_{Yi}}\cdot e^{\hat{\$}_f}\cdot \\ &\quad e^{z\hat{\$}_{Zs}}\cdot e^{\hat{\$}_{Ze}}\cdot e^{A\hat{\$}_{As}}\cdot e^{\hat{\$}_{Ae}} \\ &= e^{-\hat{\$}_{Ce}}\cdot\left(e^{-PY_{zC}\hat{\$}_{yr}}\cdot e^{PX_{zC}\hat{\$}_{xr}}\right)\cdot e^{\gamma\hat{\$}_{Ci}}\cdot\left(e^{-PY_{zC}\hat{\$}_{yr}}\cdot e^{PX_{zC}\hat{\$}_{xr}}\right)^{-1}\cdot \\ &\quad e^{-\hat{\$}_{Xe}}\cdot\left(e^{-S_{xy}\hat{\$}_{zr}}\right)\cdot e^{-x\hat{\$}_{xi}}\cdot\left(e^{-S_{xy}\hat{\$}_{zr}}\right)^{-1}\cdot e^{-\hat{\$}_{Ye}}\cdot e^{-y\hat{\$}_{Yi}}\cdot e^{\hat{\$}_b}\cdot \\ &\quad \left(e^{-S_{yz}\hat{\$}_{xr}}\cdot e^{-S_{xz}\hat{\$}_{yr}}\right)\cdot e^{z\hat{\$}_{Zi}}\cdot\left(e^{-S_{yz}\hat{\$}_{xr}}\cdot e^{-S_{xz}\hat{\$}_{yr}}\right)^{-1}\cdot \\ &\quad e^{\hat{\$}_{Ze}}\cdot\left(e^{PY_{xA}\hat{\$}_{zr}}\cdot e^{PZ_{xA}\hat{\$}_{yr}}\right)\cdot e^{\alpha\hat{\$}_{Ai}}\cdot\left(e^{PY_{xA}\hat{\$}_{zr}}\cdot e^{PZ_{xA}\hat{\$}_{yr}}\right)^{-1}\cdot e^{\hat{\$}_{Ae}}\end{aligned} \tag{35}$$

$\hat{\$}_f = [0,0,0,0,0,0]^T$ represents the machine bed.

The tool tip error is the deviation of the ideal from the actual homogeneous coordinates of the tool tip. The error transformation matrix $\boldsymbol{E}$, can be written as:

$$\boldsymbol{E} = T_i^{-1}\cdot T_a \tag{36}$$

The three components of $\boldsymbol{E}$ are E_x, E_y and E_z.

$$[E_x, E_y, E_z, 1]^T = \mathbf{E}\cdot[0,0,0,1]^T \tag{37}$$

The installation errors of the tool and workpiece are too small and can be ignored. Therefore, they are not considered in this paper. E_x, E_y and E_z are shown by the Eqs. (38, 39), and (40), respectively.

$$\begin{aligned}E_x &= \gamma x(PY_{zC}-PX_{zC}\delta_{xC}) + \delta_{xA}-\delta_{xx}-\delta_{xy} + \delta_{zx}\varepsilon_{yx}\varepsilon_{xy}-\delta_{yy}\varepsilon_{yx}\varepsilon_{xy} \\ &\quad + x\left(S_{xy}\varepsilon_{yy} + \alpha PY_{xA}\varepsilon_{xA}\right)-\delta_{yy}\varepsilon_{xA}\varepsilon_{zx} + \left(z+\delta_{zz}+\delta_{zA}+\delta_{yz}\varepsilon_{xC}\right) \\ &\quad \left(\varepsilon_{yx}+\varepsilon_{yy}-\varepsilon_{xy}\varepsilon_{zx}\right)\left(\gamma x+\delta_{zC}+\delta_{xC}\varepsilon_{yA}\right)\left(\varepsilon_{zC}+\varepsilon_{zz}-\varepsilon_{xy}\varepsilon_{zx}\right) \\ &\quad + \varepsilon_{zx}\left(\varepsilon_{xy}\varepsilon_{yy}-\varepsilon_{zy}\varepsilon_{zA}\right)-\varepsilon_{yx}\left(\varepsilon_{yy}+\varepsilon_{xy}\varepsilon_{zy}\right) \\ &\quad -y\left(\varepsilon_{zx}+\varepsilon_{zC}+\varepsilon_{yz}\left(1-\varepsilon_{yx}\varepsilon_{yy}\right)+\varepsilon_{xy}\left(\varepsilon_{yx}\varepsilon_{yC}+\varepsilon_{yy}\varepsilon_{zx}\varepsilon_{zy}\right)\right) \\ &\quad + \left(-zS_{yz}+\delta_{yz}-\delta_{zz}\varepsilon_{xz}\right)\left(\varepsilon_{zx}+\varepsilon_{zy}\left(\varepsilon_{zA}-\varepsilon_{yx}\varepsilon_{yy}\right)+\varepsilon_{xy}\left(\varepsilon_{yx}+\varepsilon_{yy}\varepsilon_{zx}\varepsilon_{zy}\right)\right)\end{aligned} \tag{38}$$

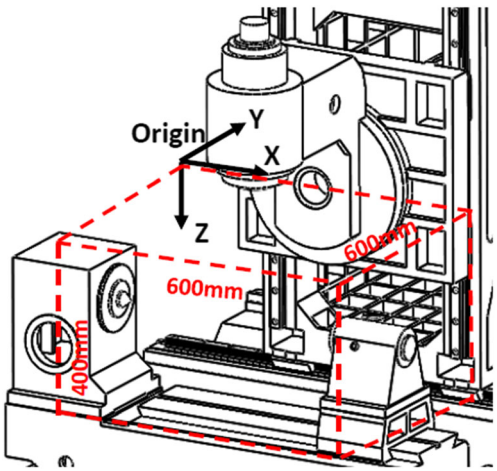

Fig. 6 Machine origin in the machine workspace

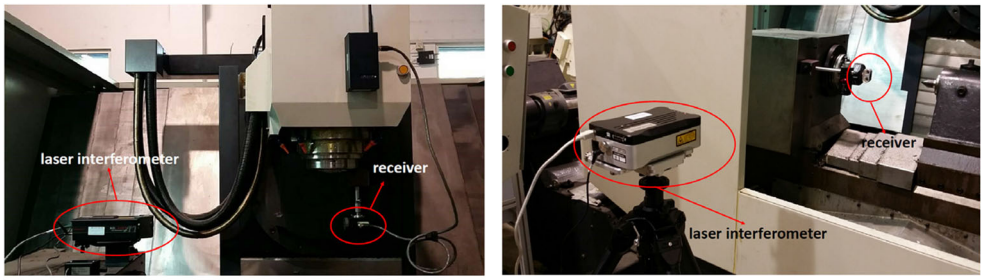

(a) Linear geometric error (b) Rotation geometric error

Fig. 7 Measurement of 30 geometric errors with laser interferometer

$$
\begin{aligned}
E_y = {} & -\delta_{yx}-\delta_{zx}\varepsilon_{xx}+\alpha y\left(\varepsilon_{yA}+PY_{xA}\right)-\gamma z\left(\varepsilon_{xA}+\varepsilon_{xC}\varepsilon_{yC}\varepsilon_{zC}\right)+\varepsilon_{xx}\left(-\delta_{zy}+\delta_{yy}\varepsilon_{xy}\right)+\\
& \left(\delta_{xy}-\delta_{zy}\varepsilon_{yA}\right)\left(\varepsilon_{xx}\varepsilon_{xC}-\varepsilon_{yA}\right)+x\left(-\varepsilon_{xx}\varepsilon_{yA}+\varepsilon_{zx}\right)+xS_{xy}\left(1-\varepsilon_{xx}\varepsilon_{yy}\varepsilon_{zx}\right)\\
& -\left(\delta_{yy}+\delta_{zy}\varepsilon_{xy}\right)\left(1+\varepsilon_{xx}\varepsilon_{yy}\varepsilon_{zx}\right)+\left(z+\delta_{zz}+\delta_{yz}\varepsilon_{xz}\right)\left(\varepsilon_{xy}+\varepsilon_{yy}\varepsilon_{xA}+\varepsilon_{xx}\left(1+\varepsilon_{yx}\left(-\varepsilon_{yy}+\varepsilon_{xy}\varepsilon_{zx}\right)\right)\right)\\
& +\left(-zS_{xz}+\delta_{xz}+\delta_{zz}\varepsilon_{zy}+\delta_{zA}\varepsilon_{yy}\right)\left(\varepsilon_{xx}\varepsilon_{yx}-\varepsilon_{zx}+\left(1+\varepsilon_{xx}\varepsilon_{yx}\varepsilon_{zx}\right)\left(\varepsilon_{xy}\varepsilon_{yy}-\varepsilon_{zy}\right)\right.\\
& \left.+\varepsilon_{xx}\left(\varepsilon_{yy}+\varepsilon_{xy}\varepsilon_{zC}\right)\right)-y\left(\varepsilon_{zy}\left(\varepsilon_{xx}\varepsilon_{yx}-\varepsilon_{zx}\right)+\varepsilon_{xx}\left(-\varepsilon_{xy}+\varepsilon_{yy}\varepsilon_{zA}\right)+\left(1+\varepsilon_{xx}\varepsilon_{yC}\varepsilon_{zy}\right)\left(1+\varepsilon_{xy}\varepsilon_{xC}\varepsilon_{zx}\right)\right)\\
& +\left(-zS_{yz}+\delta_{yz}-\delta_{zz}\varepsilon_{xz}\right)\left(\left(\varepsilon_{xA}\varepsilon_{yA}-\varepsilon_{zA}\right)\varepsilon_{zy}+\varepsilon_{xx}\left(-\varepsilon_{xy}+\varepsilon_{yy}\varepsilon_{zy}\right)+\left(1+\varepsilon_{xx}\varepsilon_{yx}\varepsilon_{zx}\right)\left(1+\varepsilon_{xy}\varepsilon_{yy}\varepsilon_{zy}\right)\right)
\end{aligned}
\tag{39}
$$

$$
\begin{aligned}
E_z = {} & \delta_{zz}-\delta_{zx}-\delta_{zy}+\delta_{yx}\varepsilon_{xx}+\alpha z\left(\varepsilon_{zC}+\varepsilon_{xC}\varepsilon_{yC}\varepsilon_{xz}\right)-x\left(\varepsilon_{yx}+\varepsilon_{xx}\varepsilon_{zx}\right)+\left(-\delta_{xy}+\delta_{zy}\varepsilon_{xA}\right)\left(\varepsilon_{yx}+\varepsilon_{xx}\varepsilon_{zA}\right)\\
& +xS_{xy}\left(-\varepsilon_{xx}+\varepsilon_{yx}\varepsilon_{zA}\right)+\left(z+\delta_{zz}+\delta_{yz}\varepsilon_{xz}\right)\left(1+\varepsilon_{yC}\left(\varepsilon_{yy}+\varepsilon_{xy}\varepsilon_{zx}\right)-\varepsilon_{xx}\left(\varepsilon_{xy}+\varepsilon_{xA}\varepsilon_{yy}\right)\right)\\
& +\left(-zS_{xz}+\gamma PZ_{xA}\left(\delta_{xz}+\delta_{zC}\varepsilon_{yz}\right)\right)\left(\varepsilon_{yx}+\varepsilon_{yy}+\varepsilon_{xx}\varepsilon_{zx}+\left(-\varepsilon_{xx}+\varepsilon_{xy}\varepsilon_{zx}\right)\left(\varepsilon_{xy}\varepsilon_{yy}-\varepsilon_{zy}\right)+\varepsilon_{xy}\varepsilon_{zC}\right)\\
& -y\left(-\varepsilon_{xy}+\varepsilon_{yy}\varepsilon_{zy}+\varepsilon_{xC}\left(\varepsilon_{yA}+\varepsilon_{xx}\varepsilon_{zx}\right)+\left(-\varepsilon_{xx}+\varepsilon_{yx}\varepsilon_{zx}\right)\left(1+\varepsilon_{xy}\varepsilon_{yy}\varepsilon_{zy}\right)\right)\\
& +\left(-zS_{yz}+\delta_{yz}-\delta_{zC}\varepsilon_{xz}\right)\left(-\varepsilon_{xy}+\varepsilon_{yy}\varepsilon_{zy}+\varepsilon_{zC}\left(\varepsilon_{yA}+\varepsilon_{xx}\varepsilon_{zx}\right)+\left(-\varepsilon_{xx}+\varepsilon_{yx}\varepsilon_{zx}\right)\left(1+\varepsilon_{xy}\varepsilon_{yy}\varepsilon_{zy}\right)\right)
\end{aligned}
\tag{40}
$$

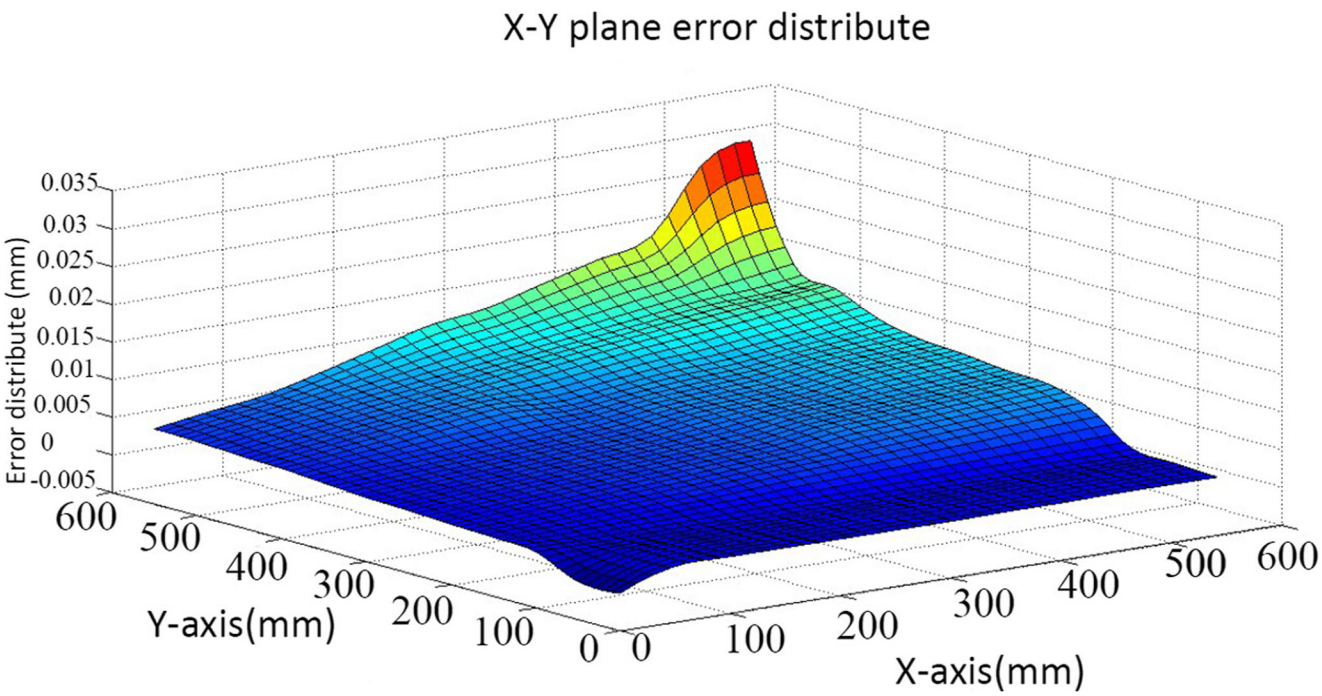

Fig. 8 Distribution of volumetric machining errors on *X*–*Y* plane

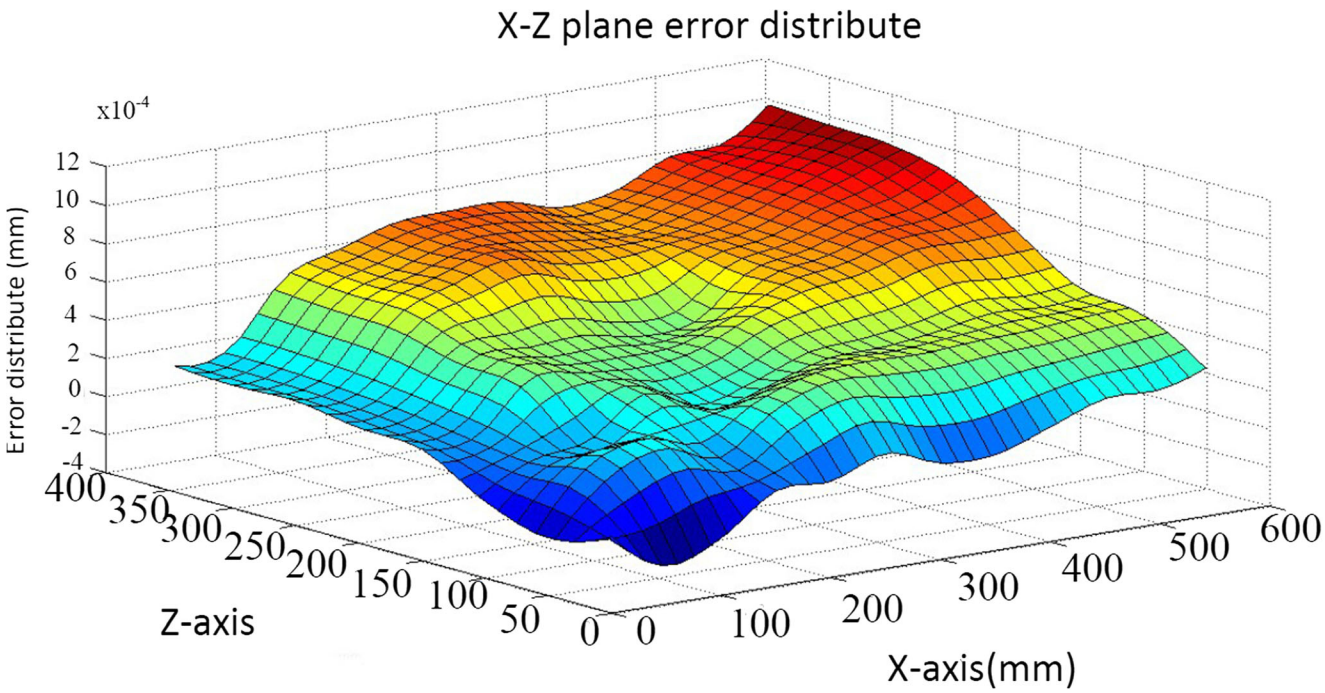

Fig. 9 Distribution of volumetric machining errors on *X–Z* plane

It should be noted that the value of geometric error (E) can be divided into two components. One is the deterministic value ($E_{\text{determine}}$) and other is the random error (Δ). As an example:

$$E = E_{\text{determine}} + \Delta$$

The E would be fluctuated around $E_{\text{determine}}$. The random part Δ cannot be compensated because of its randomness. It can be described by the rule of statistic. Cheng et al. [2] described it as Gaussian white noise.

Then, by ignoring the second and higher order error terms (for example, the term of ε_{xy}, it is multiplied by ε_{yy}, ε_{zx} and ε_{zy}

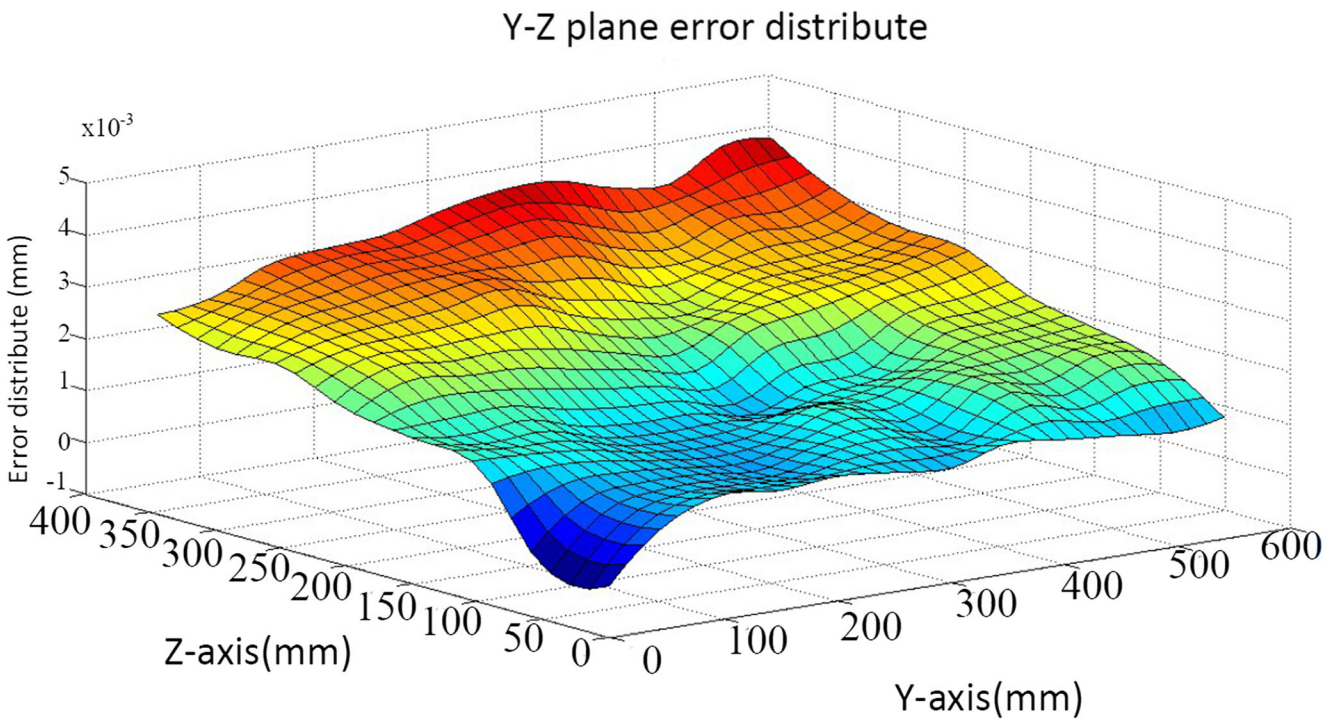

Fig. 10 Distribution of volumetric machining errors on *Y–Z* plane

Table 2 Six geometric error components of *X*-axis

Axis (mm)	0	50	100	150	200	250	300
δ_{xx} (μm)	0	−7.550	−12.130	−18.882	−24.178	−28.963	−31.998
δ_{yx} (μm)	0	−2.226	−5.613	−12.535	−20.243	−29.135	−38.138
δ_{zx} (μm)	0	1.743	3.212	7.214	9.856	12.795	15.286
ε_{xx} (μrad)	0	−1.020	−2.945	−5.682	−7.263	−9.253	−12.118
ε_{yx} (μrad)	0	6.130	6.020	5.896	5.886	5.695	5.486
ε_{zx} (μrad)	0	2.130	5.332	6.135	8.265	10.130	12.685
Axis(mm)	350	400	450	500	550	600	
δ_{xx} (μm)	−40.100	−62.152	−76.853	−85.685	−88.685	−90.152	
δ_{yx} (μm)	−43.595	−50.130	−59.155	−62.100	−75.133	−80.183	
δ_{zx} (μm)	20.283	24.137	35.200	42.400	50.145	60.853	
ε_{xx} (μrad)	−15.167	−16.690	−32.153	−39.110	−43.200	−48.163	
ε_{yx} (μrad)	5.135	4.950	4.700	4.653	4.377	4.000	
ε_{zx} (μrad)	15.162	17.009	18.593	19.165	22.130	24.000	

in Eq. (38). The results are very small and have less influence on the results, and there is not necessary to keep the higher order error terms in the final expression. Furthermore, as the comparison and simulations in Section 5.3 said, the main errors of guide rail are found who have foremost influence on the machine accuracy and they also appear in the first order model. The first order model is reduced to the following [36]:

$$\begin{aligned} E_x &= \delta_{xA} - \delta_{xx} - \delta_{xy} + \gamma x\left(PY_{zC} + \varepsilon_{zC} + \varepsilon_{zz}\right) - z S_{xz} - z\varepsilon_{yx} - z\varepsilon_{yy} - y\varepsilon_{zC} - y\varepsilon_{zx} \\ E_y &= \delta_{yz} - \delta_{yx} - \delta_{yy} + \alpha y\left(\varepsilon_{yA} + PY_{xA}\right) - \gamma y\varepsilon_{xA} + xS_{xy} - zS_{yz} + z\varepsilon_{xx} + z\varepsilon_{xy} + x\varepsilon_{zx} \\ E_z &= \quad \delta_{zz} - \quad \delta_{zx} - \quad \delta_{zy} + \quad \alpha \quad \varepsilon_{zC} - \quad x \quad \varepsilon_{yx} + \quad y \quad \varepsilon_{xx} + \quad y \quad \varepsilon_{xy} \end{aligned} \tag{41}$$

In the Eq. (38–41):

- $\boldsymbol{\alpha}$ Represents the angle of rotation of A-axis
- γ Represents the angle of rotation of C-axis
- $\boldsymbol{X}$ Represents the *X*-axis displacement
- $\boldsymbol{Y}$ Represents the *Y*-axis displacement
- $\boldsymbol{Z}$ Represents the *Z*-axis displacement.

In recent years, innumerable methods for obtaining measurements have been presented which include 22-line method [37], 15-line method [38], 12-line method, nine-line method, and the vector diagonal measurement method. In this paper, the nine-line method is applied to obtain the linear error data because identification theory

Table 3 Six geometric error components of *Y*-axis

Axis (mm)	0	50	100	150	200	250	300
δ_{xy} (μm)	0	−0.286	−1.230	−8.082	−9.008	−15.063	−18.008
δ_{yy} (μm)	0	7.580	12.150	18.000	23.685	28.695	33.595
δ_{zy} (μm)	0	0.050	0.980	1.630	9.856	12.795	15.286
ε_{xy} (μrad)	0	0.020	1.935	3.282	4.253	6.203	10.018
ε_{yy} (μrad)	0	−0.530	−0.993	−1.196	−4.056	−8.690	−12.086
ε_{zy} (μrad)	0	−0.100	−0.392	−1.160	−1.580	−2.831	−8.685
Axis(mm)	350	400	450	500	550	600	
δ_{xy} (μm)	−20.400	−22.002	−24.900	−38.605	−40.985	−52.152	
δ_{yy} (μm)	36.178	44.100	53.655	58.860	72.300	89.162	
δ_{zy} (μm)	18.203	24.137	30.110	35.030	38.155	47.853	
ε_{xy} (μrad)	13.267	20.000	30.053	25.210	33.200	48.163	
ε_{yy} (μrad)	−18.735	−23.050	−28.950	−29.653	−35.377	−38.000	
ε_{zy} (μrad)	−10.000	−12.109	−15.003	−20.000	−23.930	−25.993	

Table 4 Six geometric error components of *Z*-axis

Axis(mm)	0	50	100	150	200	250	300	350	400
δ_{xz} (μm)	0	−0.050	−0.230	−1.172	−2.008	−3.000	−5.009	−6.440	−6.906
δ_{yz} (μm)	0	0.080	0.993	1.300	1.995	2.695	2.999	3.965	4.860
δ_{zz} (μm)	0	2.750	2.980	1.306	1.866	1.095	0.468	−0.203	−1.137
ε_{xz} (μrad)	0	0	−0.535	−1.082	0	0.998	1.069	2.067	3.000
ε_{yz} (μrad)	0	−0.483	−1.093	−0.596	−1.100	−0.660	0	0.756	1.050
ε_{zz} (μrad)	0	0	0.302	0.960	1.000	1.641	2.585	2.023	3.109

of this method is not based on the geometric error model, whereas the other methods identify the error components by employing the geometric error model. Therefore, it may not be accurate to verify the integrated geometric error model using these error components. Figure 6 is a sketch showing the position of origin of the machine in machine workspace (Fig. 7). Based on the measurements shown, the volumetric machining errors on *X*–*Y* plane, *Y*–*Z* plane, and *X*–*Z* plane were calculated and are shown in Figs. 8, 9, and 10. Pictures (a) and (b) of Fig. 7 illustrate the measurement scenario of the nine-line method for identifying the 18 linear geometric error components and 12 rotation errors. The results obtained from these experiments are shown in the Tables 2, 3, 4, 5, and 6. The linear error results of the illustrated five-axis machine tool were measured with API 6D laser interferometer, and the rotary errors were measured with RENISHAW (XL80) laser interferometer. From the data in these figures, it can be seen that the volumetric machining errors increased with the distance. This result is due to the squareness errors and parallelism errors.

4 Global sensitivity analysis based on the Morris method

In the earlier work, the error modelling was established by POE screw theory. A suitable method should be employed for the analysis and to elucidate the key error terms according to the error modelling. Such approach is very important for improving machining accuracy and determining the defective components. With this as objective, for the next study, the Morris analysis method is introduced to solve the problem.

In the Morris method [28], a model parameter is changed in a large global district which influences the output result. The implementation process of this method is shown in Fig. 11. The elementary effect (***EE***) is assumed to evaluate the sensitivity of parameter φ_i, which obeys a distribute type $\boldsymbol{F_i}$. The global sensitivity of parameter can be defined by the mean $\boldsymbol{\mu}_{\text{morris}}$ and standard deviation $\boldsymbol{\sigma}_{\text{morris}}$ of the distribute type $\boldsymbol{F_i}$ (Here, the mean and standard deviation are not used for describing the real error distribution. Their functions are used to obtain the most global influencing error components). The higher the mean of the parameter φ_i, the greater is its influence on the output result. Similarly, the smaller the standard deviation of the parameter φ_i, the less is its influence on others parameters in the global system and vice versa. However, because of randomness of this method, errors in the sampling or stochastic process are caused easily. Therefore, the sample should be measured repeatedly and the averaged result obtained should be taken as the sensitivity of parameter.

The system model is set as $\boldsymbol{\varphi}=\boldsymbol{\varphi}(\theta_1,\theta_2,\theta_3,\ldots\theta_m)$. The Morris method rule states that every parameter should be normalized so that its value is in between 0 to 1 and discretized. From this process, each parameter gets a value form the group $\left\{0,\frac{1}{p-1},\frac{2}{p-1},\ldots,1\right\}$, in which, $\boldsymbol{p}$ is the number of sample of each parameter. Every parameter in the system model gets a value in the sample randomly, and vector $\boldsymbol{Z}$ consists of these parameters as shown in Eq. (42):

$$\boldsymbol{Z}=[z_1,z_2,\ldots,z_m] \tag{42}$$

In the above expression, $\boldsymbol{m}$ is the number of samples.

The variation $\boldsymbol{\Delta}$ applies on $\boldsymbol{z_i}$ in vector $\boldsymbol{Z}$. Elementary effect (***EE***) is:

$$\boldsymbol{EE}_i(\boldsymbol{Z^0})=\frac{\varphi\left(z_1^0,\ldots,z_i^0+\Delta,\ldots,z_m^0\right)-\varphi(z^0)}{\Delta} \tag{43}$$

The value of $\boldsymbol{\Delta}$ is set at $\boldsymbol{\Delta}=\frac{1}{p-1}$ in advance.

Using these rules, the process for global sensitivity analysis based on Morris method is carried out in following steps.

Step 1 The matrix $\boldsymbol{S^*}$ is diagonal, its size is $\boldsymbol{m}$, and each diagonal element is "1" or "-1" equiprobably. The

Table 5 Six geometric error components of *A*-axis

Axis (°)	0	60	120	180	240	300	360
δ_{xA} (μm)	0	0	−0.080	0	0.062	0	−0.008
δ_{yA} (μm)	0	0.030	0.089	−0.333	0	−0.695	−0.999
δ_{zA} (μm)	0	−0.046	−0.065	−1.060	−2.343	−3.152	−3.235
ε_{xA} (μrad)	0	0.422	1.735	6.072	10.000	11.998	14.069
ε_{yA} (μrad)	0	−1.083	0.093	1.596	2.100	3.560	4.000
ε_{zA} (μrad)	0	0	−1.801	−2.888	−3.000	−4.391	−5.555

Table 6 Six geometric error components of *C*-axis

Axis (°)	−80	−40	0	40	80
δ_{xC} (μm)	0	0	0	0	0
δ_{yC} (μm)	−2.000	−1.030	0	1.000	1.828
δ_{zC} (μm)	1.113	0	0	−2.333	−3.343
ε_{xC} (μrad)	0	0.333	0	1.200	1.958
ε_{yC} (μrad)	0	−1.083	0	1.596	2.100
ε_{zC} (μrad)	4.862	3.338	0	−2.969	−3.000

matrix $\boldsymbol{D}$ is lower tridiagonal and its elements are "1" and "0". $\boldsymbol{D}$ belongs to $\boldsymbol{R}^{(m+1)\times m}$.

$$\boldsymbol{D}=\begin{bmatrix} 0 & 0 & 0 & \cdots & 0 \\ 1 & 0 & 0 & \cdots & 0 \\ 1 & 1 & 0 & \cdots & 0 \\ \vdots & \vdots & \vdots & \ddots & \vdots \\ 1 & 1 & 1 & 1 & 0 \end{bmatrix}$$

$\boldsymbol{A_{l,m}}$ is the unit matrix the size of which is $(l\times m)$, and $l=m+1$. Then, the size of matrix $\boldsymbol{A}^*=(2\mathbf{D}-A_{i,m})\mathbf{S}^*+A_{i,m}$ is $(l\times m)$. Moreover, every element in matrix $\boldsymbol{A}^*$ is equal to the corresponding element in the matrix $\boldsymbol{D}$,or "0" transforms to "1"and "1" transforms to "0".

Step 2 $\boldsymbol{\theta}^*$ is the base value for input parameters $\boldsymbol{\theta}$, and each parameter gets a value from the group $\left\{0,\frac{1}{p\text{-}1},\frac{2}{p\text{-}1},\ldots,1\right\}$ randomly.

Step 3 $\boldsymbol{W}^*$ is the permutation matrix the size of which is $(m\times m)$. There is only one element with value "1" in each line or row in this matrix; other elements are "0". The randomized matrix $\boldsymbol{D}^*$ of sample matrix $\boldsymbol{D}$ is as shown in Eq. (44):

$$\boldsymbol{D}^*=\left[A_{m+1,1}\theta^*+\left(\Delta/2\right)A^*\right]W^* \tag{44}$$

The matrices $\mathbf{S}^*$, $\boldsymbol{\Theta}^*$ and $\mathbf{W}^*$ are stochastic and independent. The matrix $\boldsymbol{D}^*$ also is randomized. Moreover, there is only single value difference between every two rows in the matrix $\boldsymbol{D}^*$ and considering the rank j as an example.

$$\boldsymbol{D}(j)=\begin{bmatrix} \theta_1 & \cdots & \theta_{j1} & \cdots & \theta_m \\ \theta_1 & \cdots & \theta_{j2} & \cdots & \theta_m \end{bmatrix} \tag{45}$$

Here, $\theta_{j1}-\theta_{j2}=\Delta$, and $\boldsymbol{D}(j)$ is chosen as the input parameter vector. The element j is of "$\boldsymbol{EE}$" and can be calculated basing on Eq. (46).

$$\boldsymbol{EE}_j=\frac{\varphi(\theta_1,\ldots,\theta_{j1},\ldots,\theta_m)-\varphi(\theta_1,\ldots,\theta_{j2},\ldots,\theta_m)}{\Delta} \tag{46}$$

The entire adjacent rows of elements are the input parameters in this system. The "$\boldsymbol{EE}$" of all parameters is calculated using this procedure, especially for the complex geometric errors with higher efficiency.

Step 4 According to the sampling number n, steps 1 to 3 should be carried out for n times. With a counting process, $\boldsymbol{EE}$ value of every parameter can be calculated.

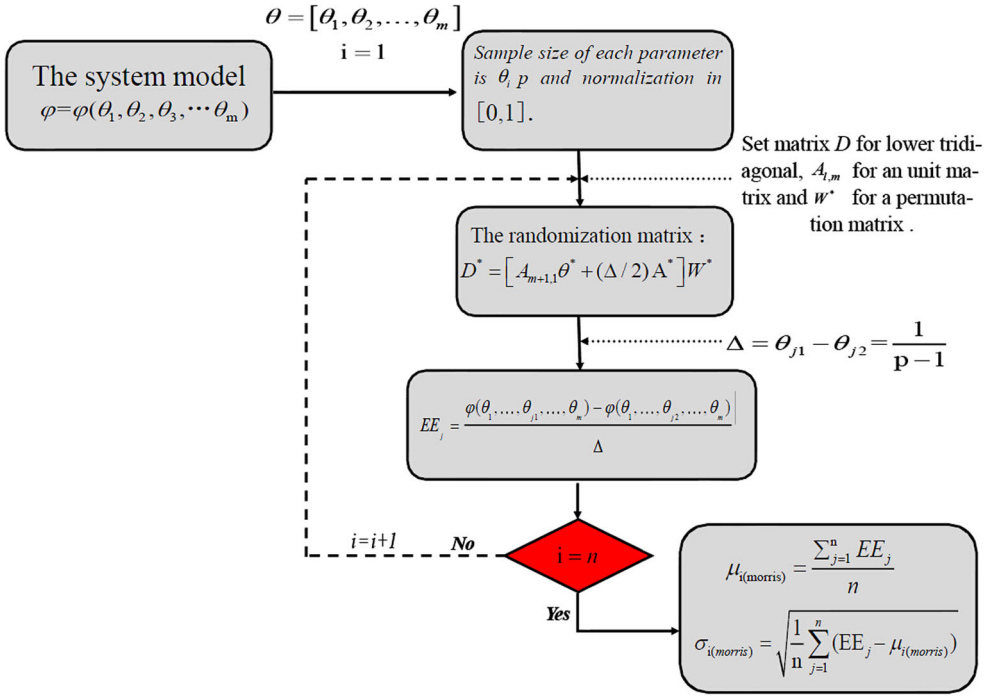

Fig. 11 Process of Morris method in global sensitivity analysis

Fig. 12 Uniform distribution of *X*-axis errors by Modified Morris Method

Step 5 Calculate the mean and standard deviation of the ***EE*** with θ as input parameter.

$$\mu_{i(\text{morris})} = \frac{\sum_{j=1}^{n} EE_j}{n}$$

$$\sigma_{\text{i(morris)}} = \sqrt{\frac{1}{\text{n}}\sum_{j=1}^{n}\left(EE_j - \mu_{i(\text{morris})}\right)}$$

Step 6 Make a judgment on the global sensitivity for input parameters.

5 Global sensitivity analysis and modification

5.1 The modification for process of Morris

According the POE modelling of screw theory for volumetric machining errors, the error models on *X*-, *Y*-, and *Z*-axis of the

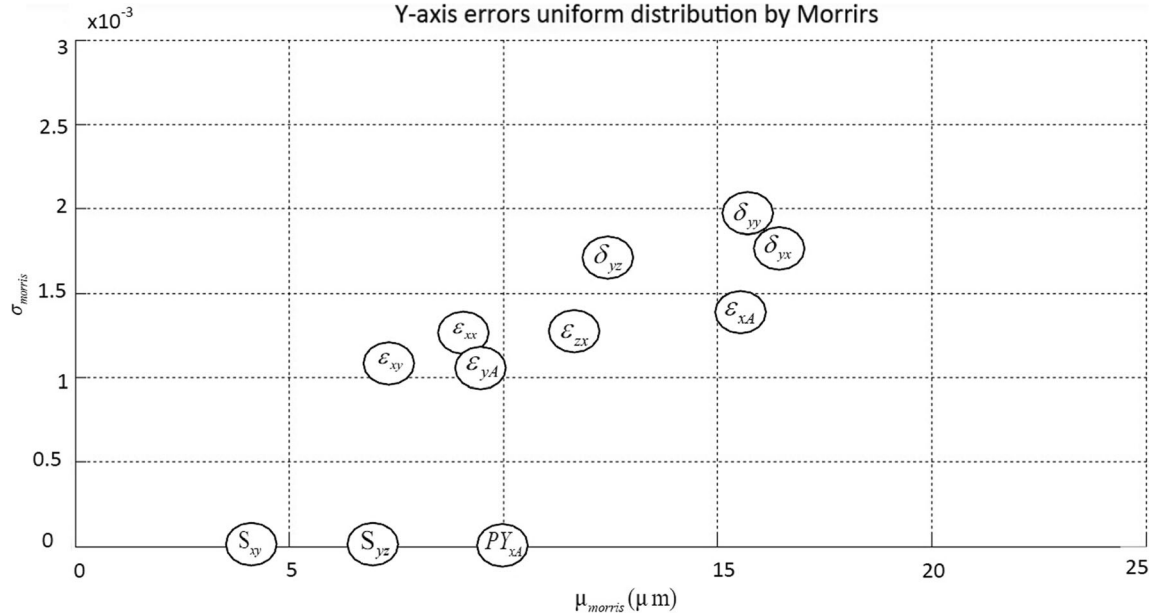

Fig. 13 Uniform distribution of *Y*-axis errors by Modified Morris Method

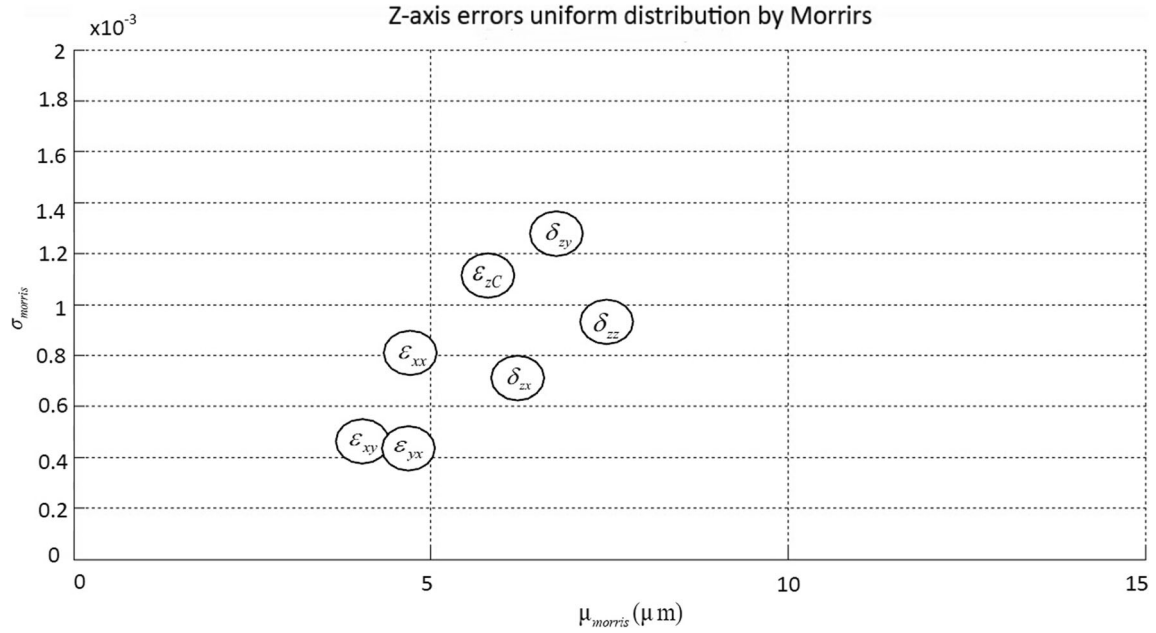

Fig. 14 Uniform distribution of *Z*-axis errors by Modified Morris Method

five-axis machine tool are shown in Eq. (47) to Eq. (49):

$$\boldsymbol{E_x} = \boldsymbol{f}\left(\delta_{xA}, \delta_{xx}, \delta_{xy}, PY_{zC}, \varepsilon_{zC}, \varepsilon_{zz}, S_{xz}, \varepsilon_{yx}, \varepsilon_{yy}, \varepsilon_{zx}\right) \quad (47)$$

$$\boldsymbol{E_y} = \boldsymbol{g}\left(\delta_{yz}, \delta_{yx}, \delta_{yy}, \varepsilon_{yA}, PY_{xA}, \varepsilon_{xA}, S_{xy}, S_{yz}, \varepsilon_{xx}, \varepsilon_{xy}, \varepsilon_{zx}\right) \quad (48)$$

$$\boldsymbol{E_z} = \boldsymbol{\varphi}\left(\delta_{zz}, \delta_{zx}, \delta_{zy}, \varepsilon_{zC}, \varepsilon_{yx}, \varepsilon_{xx}, \varepsilon_{xy}\right) \quad (49)$$

There are 25 error terms that mostly affect the volumetric machining errors and these include 10 parameters on the *X*-axis, 11 parameters on *Y*-axis, and 7 parameters on *Z*-axis. There are 3 repetitive terms.

Considering the measured data of geometric errors on *X*-axis as an example, the true value of every error term $\boldsymbol{L_i}$ (i=1, 2,3,…,11) is *C* and is normalized as:

$$\boldsymbol{z_i} = \frac{|C_i|}{\sum_{1}^{10} |C|_i} \quad (50)$$

The range of $\boldsymbol{L_i}$ is from 0 to 1, and belongs to uniform distribution. To shrink the range, the $\boldsymbol{p}$ should be even, and the variation is $\boldsymbol{\Delta} = \frac{\mathrm{p}}{2(p-1)}$. The **Step 2** and **Step 3** described earlier should be modified in Morris method according to the procedure shown below.

Modified Step 2 $\boldsymbol{L}^*$ is the base value for the input parameters $\boldsymbol{L}$ and each parameter can get a value from $\left\{0, \frac{1}{\mathrm{p\text{-}1}}, \frac{2}{\mathrm{p\text{-}1}}, \ldots, 1\text{-}\Delta\right\}$ randomly.

Modified Step 3 The $\boldsymbol{W}^*$ is the permutation matrix of size ($m \times m$). There is only one element with value "1" in each line or row in this matrix, and rest are "0".

$$D^* = \left[A_{m+1,1}\theta^* + \left(\Delta/2\right)A^*\right]W^*$$

Here, $\theta_{j1} - \theta_{j2} = \Delta$, and $D(j)$ is chosen as the input parameter vector. The element $\boldsymbol{j}$ is of "$\boldsymbol{EE}$" and can be calculated using the following relationship:

$$\boldsymbol{EE}_j = \frac{\sqrt{\sum \left[f_{\mathrm{axis}}(L_1, \ldots, L_{j1}, \ldots, L_{10}) - f_{axis}(L_1, \ldots, L_{j2}, \ldots, L_{10})\right]^2}}{\Delta} \quad (51)$$

In the above, $f_{\mathrm{axis}}(\bullet)$ represents the output geometric errors on X-axis with the element *j*.

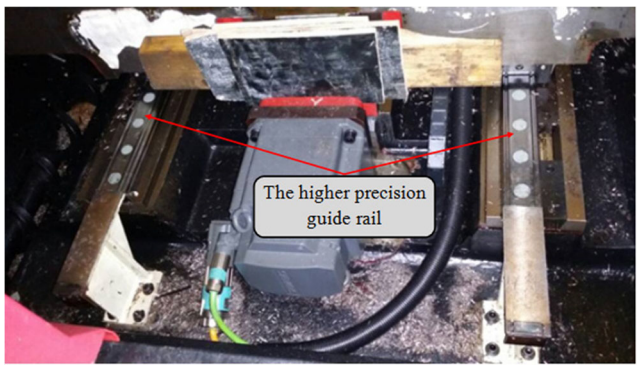

Fig. 15 Guide rail modification for obtaining higher precision

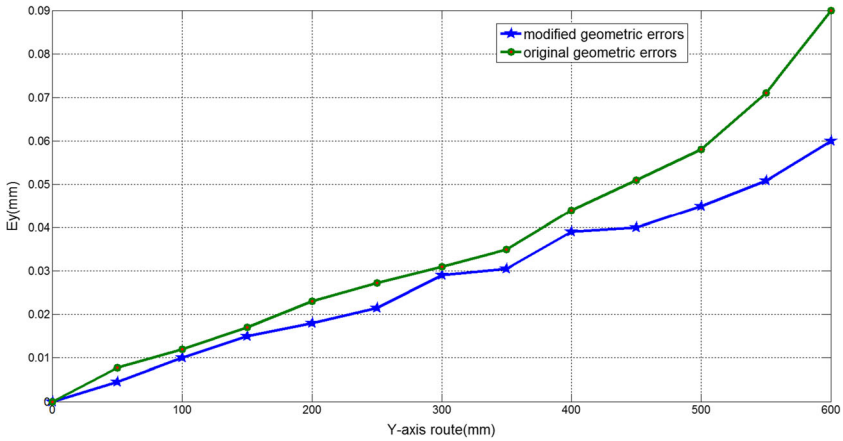

Fig. 16 Comparison of E_y for the original and modified guide rails

5.2 The global sensitivity analysis by modified Morris method

Finally, the global sensitivity can be calculated using steps 4–6. For this process, $\boldsymbol{p}$ is set as 16, and sampling times are 500. The results from global sensitivity analysis obtained on *X*-axis with Morris method are shown in Fig. 12. ($\boldsymbol{e}_l$ is $x \times cos(\boldsymbol{e}_i)$, and its unit is μm).

By using similar procedure, the results of global sensitivity on *Y*-axis and *Z*-axis were determined and shown in Figs. 13 and 14.

In this study, the mean μ_{morris} of geometric errors on the *X*-axis, namely E_x, is calculated according to the modelling calculation process. The global sensitivity order of degree of influence for the key geometric errors in E_x is: $\delta_{yz}\rangle\delta_{yy}\rangle\varepsilon_{xA}\rangle\delta_{yx}\rangle\varepsilon_{zx}\rangle PY_{zC}\rangle\varepsilon_{yA}\rangle\varepsilon_{xx}\rangle\varepsilon_{xy}\rangle S_{yz}\rangle S_{xy}$. In view of the standard deviation σ_{morris}, the top three key geometric errors on X-axis which interact with other geometric errors relatively to a larger degree are: $\varepsilon_{zC}, \delta_{xx}$ and ε_{yy}. These error terms should be controlled primarily.

Similarly, the global sensitivity order of degree of influence for the key geometric errors in E_y according to the magnitude of mean μ_{morris} is: $\delta_{yz}\rangle\delta_{yy}\rangle\varepsilon_{xA}\rangle\delta_{yx}\rangle\varepsilon_{zx}\rangle PY_{xA}\rangle\varepsilon_{yA}\rangle\varepsilon_{xx}\rangle\varepsilon_{xy}\rangle S_{yz}\rangle S_{xy}$. In view of the standard deviation σ_{morris}, the top three key geometric errors on *Y*-axis which interact with others relatively to a larger extent are: δ_{yy}, δ_{yx} and δ_{yz}. These error terms should be controlled primarily and all these impact the accuracy of Y-axis guide rail. As for the E_z, the global sensitivity order of degree of influence for the key geometric errors according the magnitude of mean μ_{morris} is: $\delta_{zz}\rangle\delta_{zy}\rangle\delta_{zx}\rangle\varepsilon_{zC}\rangle\varepsilon_{xx}\rangle\varepsilon_{yx}\rangle\varepsilon_{xy}$. In the view of the standard deviation σ_{morris}, the top three key geometric errors on Z-axis which interact with others to a greater extent are: $\delta_{zy}, \varepsilon_{zC}$ and δ_{zz}. The eight key error terms should be controlled primarily in order to improve the volumetric machining accuracy.

5.3 Verification and simulation based on GSA results

Because the squareness errors and parallelism errors PY_{zC}, S_{xz}, PY_{xA}, S_{yz} and S_{xy} are system errors, they have less influence on the other error terms. According to the results of global sensitivity analysis, the volumetric machining error of *Y*-axis mainly depends on the precision grade of guide rail on *Y*-axis. Therefore, the guide rails on *Y*-axis are replaced by two other rails with higher precision, as shown in Fig. 15. The geometric errors are measured after this modification. By the volumetric machining accuracy model, Fig. 16 shows the E_y under the original and modified conditions of the machine tool. It can be

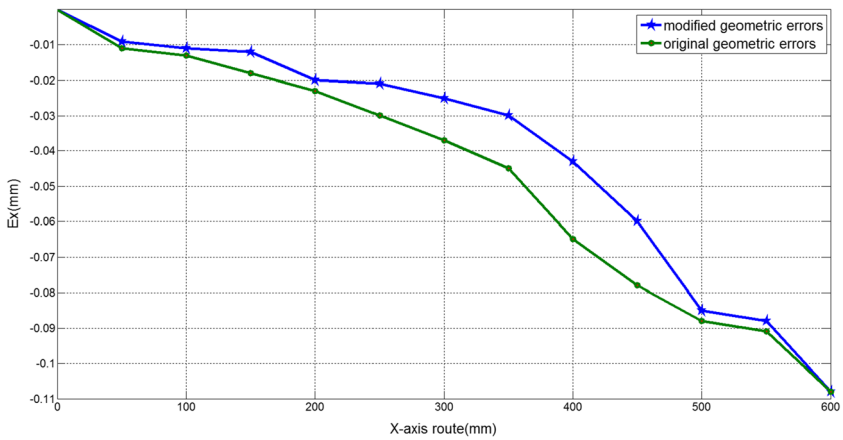

Fig. 17 Simulation results of E_x for original and modified guide rails

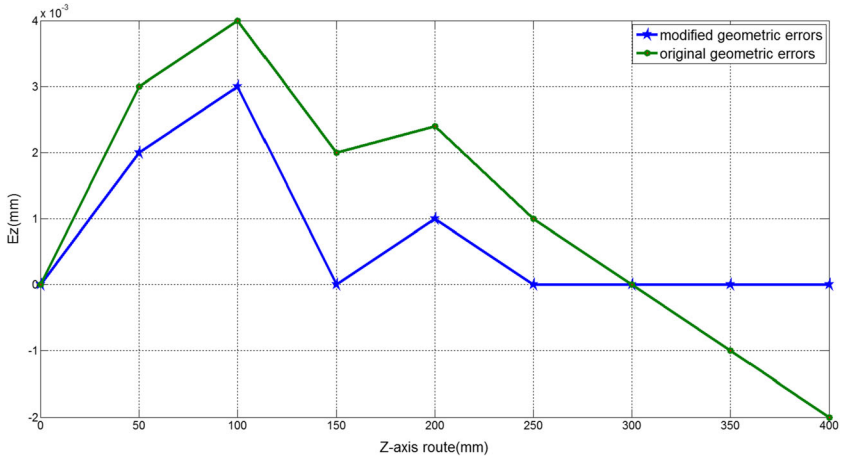

Fig. 18 Simulation results of E_z for original and modified guide rails

seen that the E_y is obviously reduced with the modified guide rails.

The methodology has a wide-range of practical applicability. A simulation was carried out as a proof. An assumption is made that the key components of five-axis machine tools are replaced according to the results of methodology. These key components are those that can lead to key geometric errors mostly affecting the machining accuracy. After replacement, the key geometric errors were reduced by 20 %. Figures 17 and 18 show that space errors E_x and E_z clearly decreased.

Therefore, on the basis of experimental and simulation results obtained, it can be stated that the POE of screw theory modelling and Morris method global sensitivity analysis are very useful tools and can be widely applied to improve the machining accuracy of a machine tool.

6 Conclusion

In this research, based on the POE screw theory, a method was established to model the volumetric machining accuracy of a five-axis machine tool. The formulae for geometric errors on *X*-, *Y*-, and Z-axis were established, and then by ignoring the second and higher order error terms, the relationships for volumetric machining errors E_x, E_y, E_z were developed. After measuring the geometric errors by nine-line method, the volumetric machining error distributions on *X*–*Y*, *Y*–Z, and *X*–*Z* plane were established.

In view of the fact that 37 geometric errors were involved in intercoupling, in this paper, a modified Morris method was used to perform global sensitivity analysis and identify the key error terms having a greater influence on the volumetric machining error. The results indicated that the Morris mean affects the output results, and that Morris standard deviation represents the degree of influence.

Of course, besides the geometric errors, thermal and load-induced errors also lower the volumetric machining accuracy of a machine tool. Therefore, in future research, in order to improve machining accuracy further, the authors hope to pursue the sensitivity analysis of machining accuracy by taking more error sources into consideration.

Acknowledgments The authors are extremely grateful to National Natural Science Foundation of China (No.51575010) Beijing Nova Program (Z151100000315013 8), The Leading Talent Project of Guangdong Province, Open Project of State Key Lab of Digital Manufacturing Equipment & Technology (Huazhong University of Science and Technology), and Shantou Light Industry Equipment Research Institute of science and technology Correspondent Station (2013B090900008), for supporting the research presented in this paper.

References

1. Kvrgic V, Dimic Z, Cvijanovic V, Ilic D, Bucan M (2012) A control algorithm for a vertical five-axis turning centre. Int J Adv Manuf Technol 61(5-8):569–584
2. Cheng Q, Feng Q, Liu Z, Gu P, Cai L (2014) Fluctuation prediction of machining accuracy for multi-axis machine tool based on stochastic process theory. Proc Inst Mech Eng C J Mech Eng Sci 0954406214562633
3. Hong C, Ibaraki S, Matsubara A (2011) Influence of position-dependent geometric errors of rotary axes on a machining test of cone frustum by five-axis machine tools. Precis Eng 35(1):1–11
4. Liu H, Li B, Wang X, Tan G (2011) Characteristics of and measurement methods for geometric errors in CNC machine tools. Int J Adv Manuf Technol 54(1-4):195–201
5. Schwenke H, Knapp W, Haitjema H, Weckenmann A, Schmitt R, Delbressine F (2008) Geometric error measurement and compensation of machines—an update. CIRP Ann-Manuf Technol 57(2): 660–675
6. Ziegert JC, Kalle P (1994) Error compensation in machine tools: a neural network approach. J Intell Manuf 5(3):143–151
7. Wang J, Guo J (2013) Algorithm for detecting volumetric geometric accuracy of NC machine tool by laser tracker. Chin J Mech Eng 26(1):166–175
8. Ramesh R, Mannan MA, Poo AN (2000) Error compensation in machine tools—a review: Part I: geometric, cutting-force induced and fixture-dependent errors. Int J Mach Tools Manuf 40(9):1235–1256
9. Lamikiz A, De Lacalle LL, Ocerin O, Díez D, Maidagan E (2008) The Denavit and Hartenberg approach applied to evaluate the

consequences in the tool tip position of geometrical errors in five-axis milling centres. Int J Adv Manuf Technol 37(1-2):122–139
10. de Lacalle NL, Mentxaka AL (Eds.) (2008) Machine tools for high performance machining. Springer Science & Business Media
11. Kvrgic V, Dimic Z, Cvijanovic V, Vidakovic J, Kablar N (2014) A control algorithm for improving the accuracy of five-axis machine tools. Int J Prod Res 52(10):2983–2998
12. Tian W, Gao W, Zhang D, Huang T (2014) A general approach for error modeling of machine tools. Int J Mach Tools Manuf 79:17–23
13. Fu G, Fu J, Xu Y, Chen Z (2014) Product of exponential model for geometric error integration of multi-axis machine tools. Int J Adv Manuf Technol 71(9-12):1653–1667
14. Rahman M, Heikkala J, Lappalainen K (2000) Modeling, measurement and error compensation of multi-axis machine tools. Part I: theory. Int J Mach Tools Manuf 40(10):1535–1546
15. Eman KF, Wu BT, DeVries MF (1987) A generalized geometric error model for multi-axis machines. CIRP Ann-Manuf Technol 36(1):253–256
16. Schiehlen W (1997) Multibody system dynamics: roots and perspectives. Multibody Syst Dyn 1(2):149–188
17. Fan JW, Guan JL, Wang WC, Luo Q, Zhang XL, Wang LY (2002) A universal modeling method for enhancement the volumetric accuracy of CNC machine tools. J Mater Process Technol 129(1): 624–628
18. Chen IM, Yang G, Tan CT, Yeo SH (2001) Local POE model for robot kinematic calibration. Mech Mach Theory 36(11):1215–1239
19. Moon SK, Moon YM, Kota S, Landers RG (2001) Screw theory based metrology for design and error compensation of machine tools. In Proceedings of DETC, 1;697–707
20. Nojedeh MV, Habibi M, Arezoo B (2011) Tool path accuracy enhancement through geometrical error compensation. Int J Mach Tools Manuf 51(6):471–482
21. Xu C, Gertner G (2007) Extending a global sensitivity analysis technique to models with correlated parameters. Comput Stat Data Anal 51(12):5579–5590
22. Saltelli A, Ratto M, Tarantola S, Campolongo F, Commission E (2006) Sensitivity analysis practices: Strategies for model-based inference. Reliab Eng Syst Saf 91(10):1109–1125
23. Sudret B (2008) Global sensitivity analysis using polynomial chaos expansions. Reliab Eng Syst Saf 93(7):964–979
24. Shahsavani D, Grimvall A (2011) Variance-based sensitivity analysis of model outputs using surrogate models. Environ Model Softw 26(6):723–730
25. Nossent J, Elsen P, Bauwens W (2011) Sobol'sensitivity analysis of a complex environmental model. Environ Model Softw 26(12): 1515–1525
26. Tsutsumi M, Saito A (2003) Identification and compensation of systematic deviations particular to 5-axis machining centers. Int J Mach Tools Manuf 43(8):771–780
27. Cheng Q, Wu C, Gu P, Chang W, Xuan D (2013) An analysis methodology for stochastic characteristic of volumetric error in multiaxis CNC machine tool. Math Probl Eng 2013
28. Morris MD (1991) Factorial sampling plans for preliminary computational experiments. Technometrics 33(2):161–174
29. Campolongo F, Cariboni J, Saltelli A (2007) An effective screening design for sensitivity analysis of large models. Environ Model Softw 22(10):1509–1518
30. King DM, Perera BJC (2013) Morris method of sensitivity analysis applied to assess the importance of input variables on urban water supply yield–a case study. J Hydrol 477:17–32
31. Touhami HB, Lardy R, Barra V, Bellocchi G (2013) Screening parameters in the Pasture Simulation model using the Morris method. Ecol Model 266:42–57
32. Ruano MV, Ribes J, Seco A, Ferrer J (2012) An improved sampling strategy based on trajectory design for application of the Morris method to systems with many input factors. Environ Model Softw 37:103–109
33. Herman JD, Kollat JB, Reed PM, Wagener T (2013) Technical note: method of Morris effectively reduces the computational demands of global sensitivity analysis for distributed watershed models. Hydrol Earth Syst Sci 17(7):2893–2903
34. Li Y, Zhu M, Li Y (2006) Kinematics of reconfigurable flexible-manipulator using a local product-of-exponentials formula. In Intelligent Control and Automation, 2006. WCICA 2006. The Sixth World Congress on, 2; 9022-9026. IEEE
35. He R, Zhao Y, Yang S, Yang S (2010) Kinematic-parameter identification for serial-robot calibration based on POE formula. Robot IEEE Trans 26(3):411–423
36. Liu W, Liang M (2008) Multi-objective design optimization of reconfigurable machine tools: a modified fuzzy-Chebyshev programming approach. Int J Prod Res 46(6):1587–1618
37. Zhang G, Ouyang R, Lu B, Hocken R, Veale R, Donmez A (1988) A displacement method for machine geometry calibration. CIRP Ann-Manuf Technol 37(1):515–518
38. Chen G, Yuan J, Ni J (2001) A displacement measurement approach for machine geometric error assessment. Int J Mach Tools Manuf 41(1):149–161